RSC Medicinal Chemistry

ROYAL SOCIETY OF CHEMISTRY

RESEARCH ARTICLE

View Article Online
View Journal

Cite this: DOI: 10.1039/d0md00104j

G-Protein biased opioid agonists: 3-hydroxy-*N*-phenethyl-5-phenylmorphans with three-carbon chain substituents at C9†

Eugene S. Gutman,[a] Eric Bow,[a] Fuying Li,‡[a] Agnieszka Sulima,[a] Sophia Kaska,[b] Rachel Crowley,[c] Thomas E. Prisinzano,[bc] Yong-Sok Lee,[d] Sergio A. Hassan,[d] Gregory H. Imler,[e] Jeffrey R. Deschamps,[e] Arthur E. Jacobson *[a] and Kenner C. Rice*[a]

A series of compounds have been synthesized with a variety of substituents based on a three-carbon chain at the C9-position of 3-hydroxy-*N*-phenethyl-5-phenylmorphan (3-(2-phenethyl-2-azabicyclo[3.3.1]-nonan-5-yl)phenol). Three of these were found to be μ-opioid receptor agonists in the inhibition of forskolin-induced cAMP accumulation assay and they did not recruit β-arrestin at all in the PathHunter assay and in the Tango assay. Compound **12** (3-((1*S*,5*R*,9*R*)-2-phenethyl-9-propyl-2-azabicyclo[3.3.1]-nonan-5-yl)phenol), **13** (3-((1*S*,5*R*,9*R*)-9-((*E*)-3-hydroxyprop-1-en-1-yl)-2-phenethyl-2-azabicyclo[3.3.1]-nonan-5-yl)phenol), and **15a** (3-((1*S*,5*R*,9*R*)-9-(2-hydroxypropyl)-2-phenethyl-2-azabicyclo[3.3.1]nonan-5-yl)phenol) were partial μ-agonists. Two of them had moderate efficacies (E_{MAX} *ca.* 65%) and one had lower efficacy, and they were *ca.* 5, 3, and 4 times more potent, respectively, than morphine *in vitro*. Computer simulations were carried out to provide a molecular basis for the high bias ratios of the C9-substituted 5-phenylmorphans toward G-protein activation.

Received 1st April 2020,
Accepted 11th June 2020

DOI: 10.1039/d0md00104j

rsc.li/medchem

Introduction

The discovery of multiple intracellular signaling cascades beyond heterotrimeric G protein activation[1] has increased our knowledge of the complexity of transduction pathways triggered by μ-opioid receptor (MOR) agonists. In addition to G_i-signaling, typical MOR agonists recruit the regulatory and signaling protein β-arrestin2, which contributes to receptor desensitization and activate distinct signaling pathways. A typical MOR agonist like morphine activates both pathways, and increasing evidence indicates β-arrestin signaling may be therapeutically relevant.[2] In β-arrestin knockout mice, antinociceptive activity of morphine is increased and the development of tolerance eliminated.[3,4] Other studies have suggested that many of the adverse effects elicited by classical opioids, such as respiratory depression, gastrointestinal effects, tolerance and dependence, were at least partially mediated through recruitment of β-arrestin.[5,6] This has spurred the development of biased agonists which preferentially activate G-protein signaling in an effort to separate the side-effects long-considered inherent to the analgesic activity of MOR agonists.

The search for analgesics devoid of side-effects has been ongoing for more than a century, with perhaps tens of thousands of opioid analogs synthesized. A sound basis for their pharmacological action that would enable the synthesis of new analgesics with fewer side-effects remains elusive. *In vivo* hot-plate or tail-flick assays have been the most reliable tools for assessing analgesic activity of novel opioids and along with animal behavioral studies, divergence from the usual effects of opioids could be reliably assessed.[7] The isolation and structural elucidation of opioid receptors now allows a more rational approach

[a] *Drug Design and Synthesis Section, Molecular Targets and Medications Discovery Branch, Intramural Research Program, National Institute on Drug Abuse, National Institute on Alcohol Abuse and Alcoholism, National Institutes of Health, Department of Health and Human Services, 9800 Medical Center Drive, Bethesda, MD 20892-3373, USA. E-mail: arthurj@nida.nih.gov, kennerr@mail.nih.gov; Fax: +1 301 217 5214; Tel: +1 301 240 5216, +1 301 217 5200*

[b] *Department of Pharmaceutical Sciences, College of Pharmacy, University of Kentucky, 789 S. Limestone Street, Lexington, Kentucky 40536, USA*

[c] *Department of Medicinal Chemistry, School of Pharmacy, University of Kansas, 1251 Wescoe Hall Drive, 4070 Malott, Lawrence, Kansas 66045, USA*

[d] *Center for Molecular Modeling, Center for Information Technology, National Institutes of Health, Department of Health and Human Services, 9800 Medical Center Drive, Bethesda, MD 20892-5624, USA*

[e] *Center for Biomolecular Science and Engineering, Naval Research Laboratory, Washington DC, 20375-0001, USA*

† Electronic supplementary information (ESI) available. CCDC 1914554. For ESI and crystallographic data in CIF or other electronic format see DOI: 10.1039/d0md00104j

‡ Research Service Division, WuXi AppTec, No. 288, Fute Middle Road, Shanghai, China, 200131

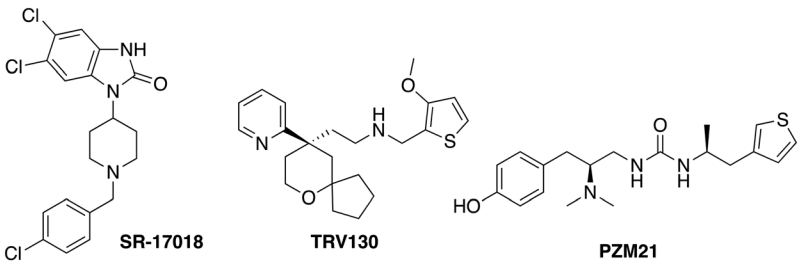

Fig. 1 G-Protein biased MOR agonists SR-17018,[12] TRV130,[5] and PZM21.[11]

to the design and synthesis of new compounds, and have given new hope that improved analgesics may eventually become available. Decades of analog synthesis provided a structurally diverse array of MOR agonists, the vast majority of which appeared to have essentially the same side-effects as morphine, although a few interesting compounds were introduced. Hot-plate and tail-flick antinociceptive assays in mice led to the introduction of pentazocine,[8] a 6,7-benzomorphan. pentazocine was found to have decreased tolerance and dependence compared to the older 4,5-epoxymorphinan and morphinan classical types of opioid and is now known to be a weak μ-antagonist, and a κ-agonist. While its clinical utility was limited due to its kappa receptor mediated dysphoric effects, it represented one of the first examples of a clinically useful opioid analgesic with decreased respiratory depression. Although the full pharmacological mechanism of action remains uncharacterized, pentazocine, along with buprenorphine, have been noted to display a "ceiling" effect on respiratory depression, wherein escalating doses beyond a certain level do not further decrease respiratory function.[9,10] With the renewed interest in opioids over the past decade, mainly due to the severe side-effects of widely available heroin and fentanyl used illicitly, new methodology and approaches have been proposed that may help identify compounds with fewer or milder side effects than those of the well-known, clinically-used analgesics. One of these approaches is based on MOR biased agonism, and several agonists with varying degrees of biased activity have recently been reported (Fig. 1).[11–13] These compounds are structurally distinct from the classical opioids based on morphine but they act primarily through the MOR and have been shown to have decreased liability for some or all of the usual opioid side-effects, *e.g.*, tolerance, constipation, and respiratory depression. All of these G-protein biased compounds recruit β-arrestin-2 to some extent.

Increased bias factor (the degree to which G-protein activation is favored over β-arrestin recruitment) has been shown to be directly correlated to enhanced analgesia without a concomitant increase in respiratory depression, widening the potential therapeutic window for these biased agonists.[12] It is still uncertain whether recruitment of β-arrestin-2 does influence respiratory depression. Recent experiments using β-arrestin-2 knockout and knockin mice suggest that β-arrestin-2 signaling does not play a role in respiratory depression.[14,15] In this study, we introduce a new series of biased compounds, namely, C9-substituted 5-phenylmorphan MOR agonists that display the highest bias factors possible for potent antinociceptive compounds. These new analogs are unable to recruit β-arrestin-2 through MOR activation and retain morphine-like or better potency.[16]

The 5-(3-hydroxy)phenylmorphans were first synthesized as structurally simpler relatives of morphine over 50 years ago by May and Murphy,[17] and remain of considerable interest for their diverse functional activity at opioid receptors. Expanding our previous study of potent analgesics bearing this template,[18] here we explore the effect of three-carbon chains at the C9 position of 5-phenylmorphans. This study includes compounds containing a three-carbon spacer between C9 and the terminal oxygen, and another with *n*-propyl at C9; some of these compounds showed equivalent or higher MOR agonist potency than morphine *in vitro* while failing to recruit β-arrestin at detectable levels. Computer simulations provided a rationale for the biased property of this series of compounds.

Results and discussion

Chemistry

Our strategy for exploring the structure–activity relationship of the C9-position on the 5-phenylmorphan scaffold relied on the previously published intermediate (±)-**1**, separable into

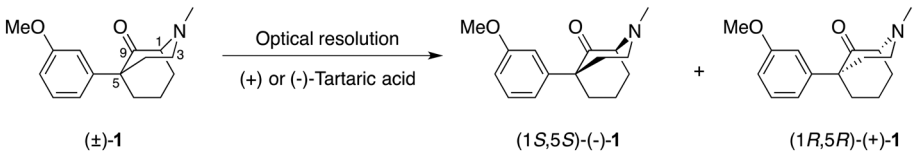

Scheme 1 Optical resolution of (±)-**1**.

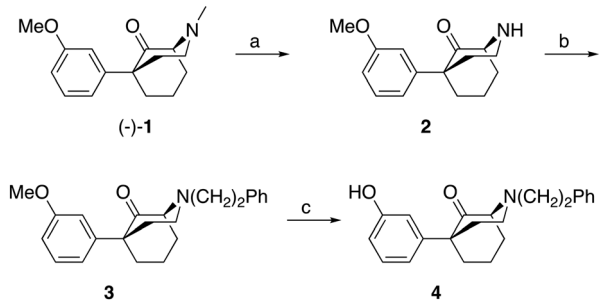

Scheme 2 Representative synthesis of intermediate **4**. Reagents and conditions: (a) CNBr, K_2CO_3, acetonitrile, rt; then 3N HCl, 100 °C, 65%; (b) 2-phenylethyl bromide, K_2CO_3, acetonitrile, 80 °C, 84%; (c) BBr_3, DCM, −78–0 °C, 94%.

enantiopure (−)-**1** and (+)-**1** through optical resolution with L-(+) and D-(−)-tartaric acid, respectively (Scheme 1).[18,19]

A small library of 5-phenymorphan compounds bearing a C9-propyl chain with and without terminal oxygen atoms were examined to probe their effect on β-arrestin recruitment and potency *in vitro*. Intermediate **4** (Scheme 2) was obtained through Von Braun demethylation of **1**, followed by alkylation and subsequent *O*-demethylation of **3** using previously described procedures (Scheme 2).[18,20]

Homologation of the C9 position was achieved in two steps through Wittig olefination and subsequent hydrolysis of the methyl vinyl ether to an epimeric mixture of aldehydes (Scheme 3). The reactivity and isomeric selectivity of both reactions were highly sensitive to the *N*-substituent, aryl functionality and hydrolysis conditions. The *E* stereochemistry of methyl vinyl ether intermediates **5**–**7** was assigned based on diagnostic NOE interaction between the C9-alkenyl and C1-methine protons.

Wittig olefination of (−)-**1** gave a 5 : 1 ratio of *E*/*Z* isomers (Scheme 3), but with the larger *N*-substituent in **3** this ratio was reversed in favor of the *Z*-isomer 1 : 4 *E*/*Z*, and reversed yet again by reaction with phenolic **4** to give a 20 : 1 ratio of *E*/*Z* isomers. The *E*/*Z* selectivity observed in this reaction is also likely to be sensitive to the conditions employed during the workup. Hydrolysis of the resultant mixtures of *E*/*Z* isomers gave varying levels of selectivity depending on the isomeric ratio and conditions (Table 1).

Hydrolysis of **7** with 3N HCl over 12 h was found to be optimal for obtaining the 1*S*,5*R*,9*R*-epimer, with longer reaction times leading to epimerization and a degradation of C9*R*-epimer selectivity. Conversion of the *Z*- to the *E*-isomer was observed during the hydrolysis of **6**; in view of the longer reaction times, this suggests that the *E*-isomer was hydrolyzed significantly faster. All attempts at chromatographic separation of the epimers generated an intensely blue colored impurity and a significant loss in yield. Therefore, the epimeric mixtures were used without any attempt at purification. Additionally, initial synthetic studies showed that late-stage *O*-demethylation of the aryl ether with either Lewis or Brønsted acids resulted in poor yields or decomposition, and thus utilizing phenol **4** as a common intermediate largely avoided these difficulties.

Using hydrolysis conditions optimized for the C9*R*-epimer, the epimeric mixture of aldehydes **10** was subjected to Horner–Wadsworth–Emmons olefination which resulted in a chromatographically separable diastereomeric mixture of enones, giving the C9*R*-epimer **11** as the major product (Scheme 4). Alternatively, Wittig olefination of **10** and immediate hydrogenation afforded propyl substituted **12**. Reduction of **11** with $LiAlH_4$ resulted in allyl alcohol **13**.

Hydrogenation of enone **11** afforded common intermediate **14**, which was reduced to propyl alcohol **15**, transesterified to ethyl ester **16**, and hydrolyzed to carboxylic acid **17** (Scheme 5). The relative configuration of the C9 position was determined by X-ray crystallographic analysis of **14b** (Scheme 5 and Fig. 2).

The C9*S*-epimer (**22**) of **14a** was synthesized in 5 steps from aldehyde **8** (Scheme 6). Horner–Wadsworth–Emmons olefination of the aldehyde gave enone **18**, *N*-demethylation to **19** resulted in a mixture of methyl and ethyl esters, which were carried forward as a mixture through the rest of the synthesis. *N*-Alkylation with phenylethyl bromide resulted in **20** and hydrogenation of the enone gave **21**. *O*-Demethylation of **21** in refluxing HBr resulted in concomitant hydrolysis of the mixture of esters; immediate esterification with MeOH and trimethyl orthoformate resulted in the methyl ester **22**.

Biological results

Given recent reports on the potential utility of G-protein biased MOR agonists, this series of compounds were evaluated for functional activity at the MOR utilizing two assays, one of which measured G-protein signaling, and in a separate assay, β-arrestin recruitment. Chinese hamster ovary cells (CHO-K1) that express human MOR (OPRM1) were used in forskolin-

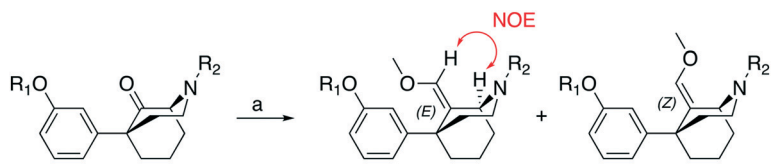

1. $R_1 = CH_3$, $R_2 = CH_3$
3. $R_1 = CH_3$, $R_2 = (CH_2)_2Ph$
4. $R_1 = H$, $R_2 = (CH_2)_2Ph$

5. *E*/*Z* = 5:1
6. *E*/*Z* = 1:4
7. *E*/*Z* = 20:1

Scheme 3 Wittig olefination of C9 carbonyl. Reagents and conditions: a. LiHMDS, (methoxymethyl)triphenylphosphonium chloride, THF, 0 °C.

Table 1 Hydrolysis of enol ethers **5**–**7**

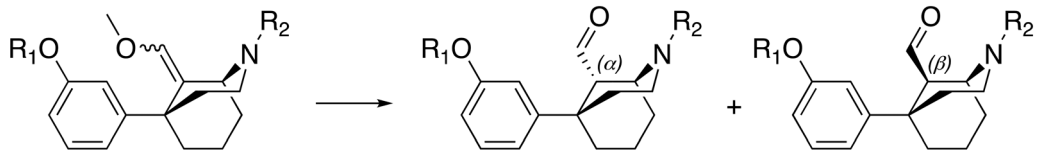

5. $R_1 = CH_3$, $R_2 = CH_3$
6. $R_1 = CH_3$, $R_2 = (CH_2)_2Ph$
7. $R_1 = H$, $R_2 = (CH_2)_2Ph$

8. $R_1 = CH_3$, $R_2 = CH_3$
9. $R_1 = CH_3$, $R_2 = (CH_2)_2Ph$
10. $R_1 = H$, $R_2 = (CH_2)_2Ph$

Cmpd	Acid	Time	$\alpha:\beta$ ratio
5 (E/Z = 5 : 1)	90% formic acid	48 h	1 : 1.5
5	aq TFA	24 h	1 : 1
5	aq $HClO_4$	24 h	1 : 1
5	3N HCl	12 h	1 : 9
5	3N HCl	24 h	1 : 2
5	6N HCl	1.5 h	1 : 3
6 (E/Z = 1 : 4)	3N HCl	36 h	1 : 3
7 (E/Z = 20 : 1)	3N HCl	12 h	1 : 7

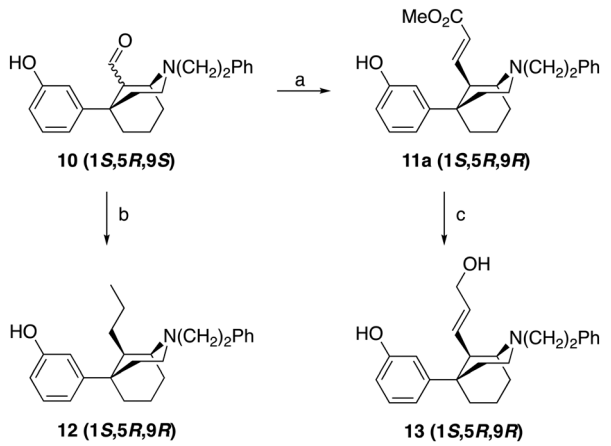

Scheme 4 Representative synthesis of analogs **11**–**13**. Reagents and conditions: (a) methyl diethylphosphonoacetate, NaH, THF, 57%; (b) ethyltriphenylphosphonium iodide, LiHMDS, THF; then 5% Pd/C, 50 psi H_2, MeOH, 28%; (c) $LiAlH_4$, THF, 0 °C, 59%.

induced cAMP assays as previously described[21] to measure functional activity through G-protein signaling (Table 2). Many of these compounds, **12**, **13**, **14a**, **15a**, were found to be potent partial agonists at MOR, while **16** was found to have low nanomolar potency at MOR as a full agonist. These compounds were also evaluated for their potency and efficacy at the human KOR (OPRK1) and DOR (OPRD1) to determine selectivity using the aforementioned forskolin-induced cAMP assay. The majority of these compounds displayed weak to no functional activity at the DOR in comparison with their EC_{50} values at MOR, and even less activity was observed at KOR. Taken together, these data suggest that these compounds are selective for activity at the MOR.

The ability of these compounds to modulate the interaction of arrestin with the MOR was also investigated in OPRM1 β-arrestin-2 cells as described previously (Table 2).[21] Bias factors were calculated in comparison to the reference ligand [D-Ala2, *N*-MePhe4, Gly-ol]-enkephalin (DAMGO) using

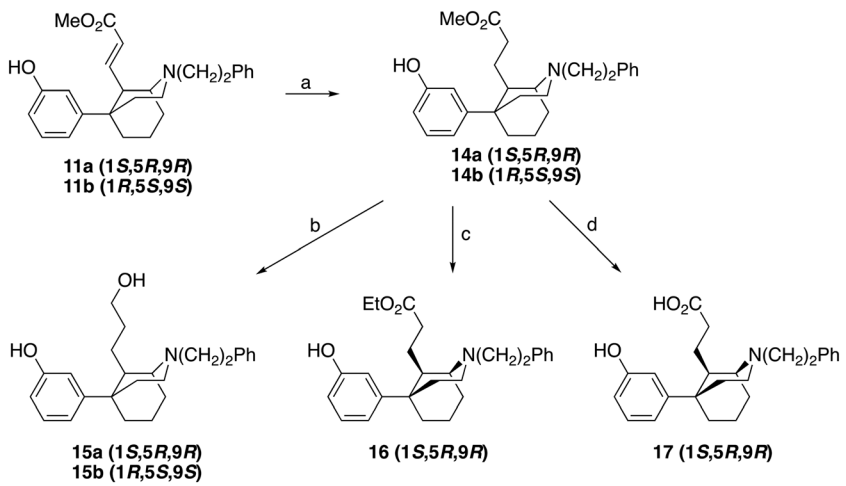

Scheme 5 Synthesis of analogs **14**–**17**. Reagents and conditions: (a) 5% Pd/C, 50 psi H_2, AcOH, MeOH, 75%; (b) $LiAlH_4$, THF, 0 °C, 88%; (c) EtOH, cat. H_2SO_4, 78 °C, 63%; (d) 1N aq LiOH, MeOH, 60 °C, 25%.

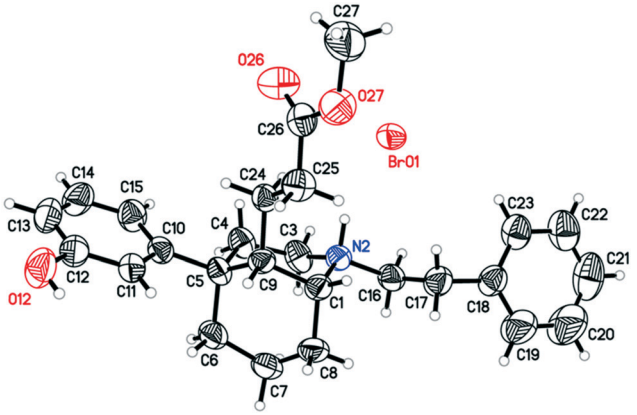

Fig. 2 X-ray crystallographic structure of methyl 3-((1*R*,5*S*,9*S*)-5-(3-hydroxyphenyl)-2-phenethyl-2-azabicyclo[3.3.1]nonan-9-yl)-propanoate hydrobromide (**14b**). The ellipsoids are shown at the 50% probability level.

previously reported methods.[22,23] A bias factor of *ca.* 1 indicates no preference for either signaling pathway and a bias factor greater than 1 indicates a bias toward G-protein signaling. The new compounds in Table 2 were compared with data obtained with these assays for the standards, morphine, SR17018 (ref. 12) and PZM21 (ref. 11) (Fig. 1), and the structurally simplest relative of the new compounds, 5-(3,9-dihydroxy)-phenylmorphan (5-(3-hydroxyphenyl)-2-phenethyl-2-azabicyclo-[3.3.1]nonan-9-ol) **23**.[18,20,24] Further investigation of signaling bias was conducted commercially through the use of a Tango GPCR assay system (Thermo Fisher Scientific).

In several instances, as shown in Table 2, bias factors were not calculable due to a lack of detectable β-arrestin2 recruitment at 25 000 nM. Compounds **11a–13** were all found to lack β-arrestin2 recruitment, with **12** and **13** showing potent partial agonist activity for G-protein mediated signaling as measured by adenylyl cyclase inhibition. Methyl and ethyl esters **14a** and **16**, respectively, showed full agonist efficacy for G-protein signaling and potent partial-agonist β-arrestin2 signaling, with bias factors lower than 2. Given that several of our potent compounds (**12**, **13**, **14b**, **15a**, **15b**, **16**, and **17**) displayed a very strong bias for the G-protein pathway utilizing an enzyme fragment complementation assay, we chose to re-evaluate β-arrestin signaling using the Tango GPCR assay,[25] an assay that does not depend on the knowledge of the G-protein signaling specificity of the MOR. The transcription-mediated response following β-arrestin recruitment relies on very specific intracellular interactions that are not altered by other signaling pathways.[26] Generally, the result on all of the compounds evaluated in the Tango GPCR assay were in agreement with the PathHunter assay results. One exception was compound **16**. While **16** had a relatively strong EC_{50} value (11.57 ± 3.1 nM), it was not very efficacious (E_{max} = 18.26 ± 1.7%). It should be noted that this level of efficacy is lower than morphine (E_{max} = 25.7 ± 0.6%) and SR 17018 (E_{max} = 89.2 ± 3.4%). Overall, extension of the carbon chain at the C9 position not only enhances the selectivity for the MOR, but also significantly reduces or completely eliminates β-arrestin recruitment.

To understand the receptor–ligand interactions responsible for the biased property, we conducted molecular dynamics (MD) simulations of compounds **12**, **14** and **15** (both 1*S*,5*R* and 1*R*,5*S* configurations) bound to the receptor. The MOR structure was taken from our previous study,[20] which contains a modeled intracellular loop 3 (ICL3, *cf.* Experimental section, ESI†). The receptor was embedded in a zwitterionic POPC membrane and solvated in a water solution with physiological concentrations of ions (see simulation setup in the Experimental section, ESI†). For comparative analysis, a simulation of the empty receptor, *i.e.*, containing only a crystallographic Na^+ ion,[27] was taken as a reference; a structure at the end of this simulation was used as the starting point for all the other simulations.

The analysis shows that the biased property of the 1*S*,5*R* series stems from strong interactions, mainly hydrophobic, between the C9 substituent and transmembrane helix 3 (TMH3) at the mid-membrane level (Fig. 3). In **12** and **15a**, the spacer and its OH substituent are critical to adopt

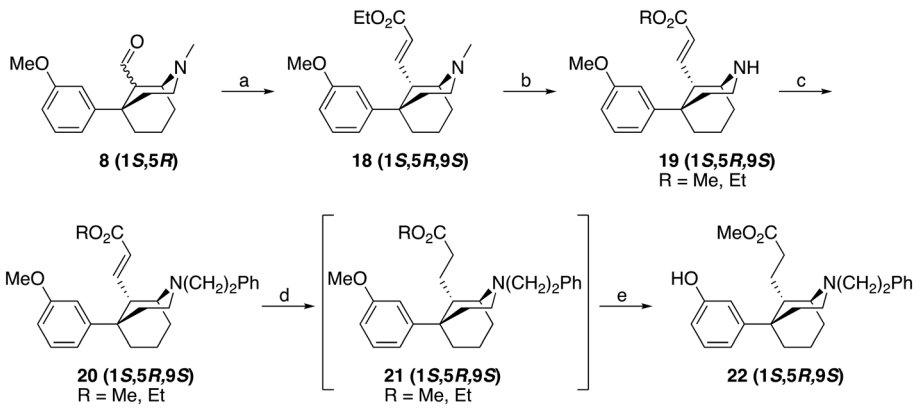

Scheme 6 Synthesis of 9*S* epimer **22**. Reagents and conditions: (a) triethylphosphonoacetate, NaH, THF, 73%; (b) 1-chloroethyl chloroformate, DCE, 80 °C; then MeOH, 60 °C, 91%; (c) 2-phenylethyl bromide, K_2CO_3, ACN, 80 °C, 68%; (d) 5% Pd/C, 50 psi H_2, MeOH, 98%; (e) 48% HBr, toluene, 120 °C; then MeOH, $HC(OMe)_3$, H_2SO_4, 60 °C, 66%.

Table 2 Inhibition of forskolin-induced cAMP accumulation: functional activity for cAMP and MOR-mediated β-arrestin2 recruitment

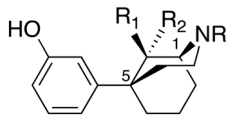

R = CH_2CH_2Ph
1*S*,5*R*

#	R_1	R_2	MOR cAMP EC_{50}[c,d] (nM)	MOR cAMP E_{MAX} %	KOR cAMP EC_{50} (nM)	KOR cAMP E_{MAX} %	DOR cAMP EC_{50} (nM)	DOR cAMP E_{MAX} %	β-Arrestin2 recruitment[a] (PathHunter assay) EC_{50} (nM)	β-Arrestin2 recruitment[a] (PathHunter assay) E_{MAX} %	β-Arrestin2 recruitment[a] (PathHunter assay) Bias factor	β-Arrestin2 recruitment[b] (Tango assay) EC_{50} (nM)	β-Arrestin2 recruitment[b] (Tango assay) E_{MAX} %	β-Arrestin2 recruitment[b] (Tango assay) Bias factor
11a	CH═CH–CO_2Me	H	132 ± 62	52.6 ± 6.5%	>10 000	—	143.0 ± 18.0	27.2 ± 3.7%	>25 000[e]	—	NC[f]	NT[g]	NT[g]	NT[g]
12	$CH_2CH_2CH_3$	H	0.95 ± 0.35	63.3 ± 3.9%	>10 000	—	>10 000	—	>25 000[e]	—	NC[f]	>25 000[e]	—	NC[f]
13	CH═CH–CH_2OH	H	2.31 ± 0.78	33.5 ± 5.9%	>10 000	—	>10 000	—	>25 000[e]	—	NC[f]	>25 000[e]	—	NC[f]
14a	CH_2CH_2–CO_2Me	H	0.46 ± 0.09	94 ± 2.3%	>10 000	—	>10 000	—	1.72 ± 0.17	4.5 ± 0.38%	0.55	12.5	123.4	0.15
15a	$CH_2CH_2CH_2OH$	H	1.2 ± 0.37	65 ± 6%	>10 000	—	80.9 ± 33.9	22.62 ± 6%	>25 000[e]	—	NC[f]	>25 000[e]	—	NC[f]
16	CH_2CH_2–CO_2Et	H	0.24 ± 0.09	100.1 ± 0.7%	35.3 ± 19.9	36.5 ± 3.8%	49.1 ± 10.1	74.2 ± 4.9%	11.57 ± 3.1	18.26 ± 1.7%	1.89	>25 000[e]	—	NC[f]
17	CH_2CH_2–CO_2H	H	31.7 ± 11.4	49 ± 2.5%	>10 000	—	>10 000	—	>25 000[e]	—	NC[f]	>25 000[e]	—	NC[f]
22	H	CH_2CH_2–CO_2Me	854 ± 114	63 ± 2.4%	322.8 ± 110.5	55.01 ± 5.0%	>10 000	—	>25 000[e]	—	NC[f]	NT[g]	NT[g]	NT[g]

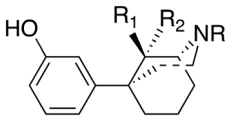

R = CH_2CH_2Ph
1*R*,5*S*

	R_1	R_2	MOR cAMP EC_{50}[c,d] (nM)	MOR cAMP E_{MAX} %	KOR cAMP EC_{50} (nM)	KOR cAMP E_{MAX} %	DOR cAMP EC_{50} (nM)	DOR cAMP E_{MAX} %	β-Arrestin2 recruitment[a] (PathHunter assay) EC_{50} (nM)	β-Arrestin2 recruitment[a] (PathHunter assay) E_{MAX} %	β-Arrestin2 recruitment[a] (PathHunter assay) Bias factor	β-Arrestin2 recruitment[b] (Tango assay) EC_{50} (nM)	β-Arrestin2 recruitment[b] (Tango assay) E_{MAX} %	β-Arrestin2 recruitment[b] (Tango assay) Bias factor
14b	H	CH_2CH_2–CO_2Me	31.3 ± 4.6	42 ± 4.8%	>10 000	—	>10 000	—	>25 000	—	NC[f]	>25 000[e]	—	NC[f]
15b	H	$CH_2CH_2CH_2$–OH	35.2 ± 12.59	48.7 ± 3.7%	>10 000	—	>10 000	—	>25 000[e]	—	NC[f]	>25 000[e]	—	NC[f]
23 (ref. 16)	H	OH[g]	0.017 ± 0.004	101%	322.8 ± 110.5	55.01 ± 5.0%	2.6 ± 0.5	74.0 ± 20.8%	6.08 ± 0.74	116 ± 5.4%	2.16	NT[h]	NT[h]	NT[h]
Standards														
Morphine			4.7 ± 0.6	103 ± 0.6%	NT[h]	NT[h]	NT[h]	NT[h]	379.6 ± 40.7	25.7 ± 0.6%	2.3	NT[h]	NT[h]	NT[h]
SR 17018[i] (ref. 12)			15.6 ± 5.1	101.2 ± 1.8%	NT[h]	NT[h]	NT[h]	NT[h]	2975 ± 1623	89.2 ± 3.4%	1.96	NT[h]	NT[h]	NT[h]
PZM21 (ref. 11)			2.5 ± 0.4	101 ± 0.6%	NT[f]	NT[f]	NT[f]	NT[f]	57.1 ± 8.5	4.3 ± 0.4%	2.98	NT[h]	NT[h]	NT[h]
Salvinorin A			NT[h]	NT[h]	0.03 ± 0.007	99.8 ± 0.3%	NT[h]	NT[h]	NT[h]	NT[h]	NT[h]	NT[h]	NT[h]	NT[h]
DADLE			NT[h]	NT[h]	NT[h]	NT[h]	0.02 ± 0.004	92.1 ± 0.7%	NT[h]	NT[h]	NT[h]	NT[h]	NT[h]	NT[h]
DAMGO			0.3 ± 0.04	101.5 ± 0.5	NT[h]	NT[h]	NT[h]	NT[h]	44.1 ± 3.9	103 ± 0.4	1.0	NT[h]	NT[h]	NT[h]

[a] HitHunter Chinese hamster ovary cells (CHO-K1) that express human μ-opioid receptor (OPRM1), human κ-opioid receptor (OPRK1), and human δ-opioid receptor (OPRD1) were used for the forskolin-induced cAMP accumulation assay to determine potency and efficacy of the compounds. PathHunter CHO cells expressing human μ-opioid receptor β-arrestin-2 EFC cells were used for the β-arrestin-2 EFC recruitment assay. All cell lines were purchased from Eurofins DiscoverX (Fremont, CA). Cell culture was performed as previously described.[21] [b] Thermo Fisher Scientific's SelectScreen™ Profiling Service: 10 point titration agonist results.[25] [c] Efficacy values were determined by normalization to DAMGO. [d] Mean ± standard error of the mean; $n \geq 2$. [e] E_{MAX} = 0% at the concentrations tested. [f] NC = not calculable. Bias factor could not be calculated because recruitment of β-arrestin2 was not observed under any of the conditions tested. [g] The C9–OH compound **23** has 1*R*,5*R*,9*S* stereochemistry.[18] [h] NT = not tested. [i] Purchased from Cayman Chemical, Ann Arbor, MI (CAS 2134602-45-0; labelled purity ≥98%), HRMS-ESI (*m*/*z*): $[M + H]^+$ calcd. for $C_{19}H_{19}Cl_3N_3O$ 410.0594, found 410.0592.

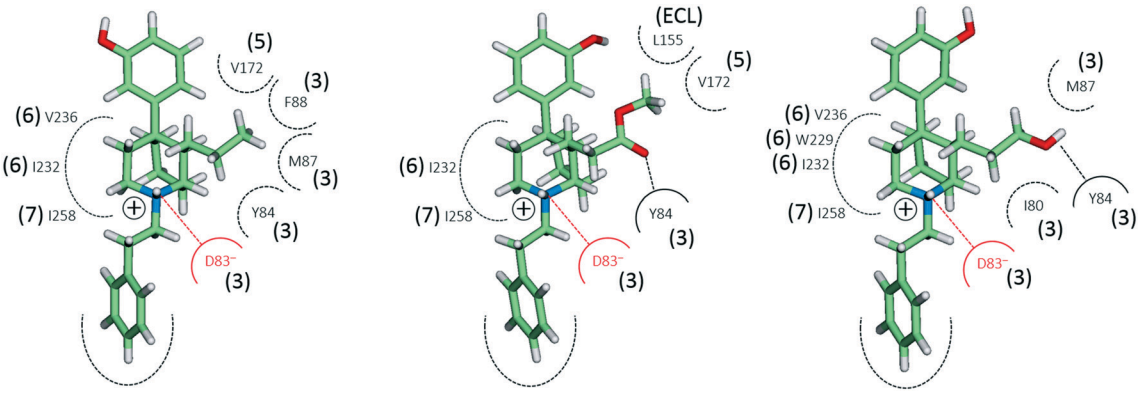

Fig. 3 From left to right, compounds **12**, **14a**, and **15a** showing the interactions of the C9 substituents with the receptor, mainly with TMH3 (helix numbers in parentheses). Hydrophobic interactions are more prevalent, but the polar groups in the chain can have important effects in its orientations, with Y84 playing a role to stabilize either the ester or hydroxy groups. Opposite to the direction of the spacer are TMH6 and TMH7 (Fig. S1†), which help stabilize the body of the ligands also through hydrophobic interactions; the head and tail of the ligands are stabilized by similar interactions in all the compounds (not shown). Not all the interactions are present simultaneously, especially in **14a**, where the H-bonding with Y84 is less frequent than in **15a**. Dashed straight lines indicate H-bonding interactions (H colored in white; C, green; N, blue; and O, red).

conformations suitable for developing these interactions. Longer chains, such as methyl ester (**14a**), bend upward, interacting with the upper residues of the receptor, including extracellular loop 2 (ECL2); the resulting weaker interactions with TMH3 appears to be ineffective in preventing β-arrestin recruitment. However, in compound **22**, the C9*S*-epimer of the methyl ester (**14a**), the chain is reoriented and regains the favorable interactions with TMH3, resulting in bias ratio comparable to **12** and **15a**. Reorienting the chain in this fashion also resulted in a dramatic loss of agonist potency at the MOR. This stereospecificity could be further exploited to design novel, highly-potent biased agonists. On the other hand, a very potent μ-agonist phenylmorphan **23** (1*R*,5*R*,9*S*) lacks a carbon spacer at the C9 position and has a bias ratio (2.2) comparable to morphine. Previous simulations[20] showed that the C9*S*–OH in **23** has little effect on the movement of TMH3, consistent with its non-biased activity; this is also the case for morphine[20] despite its different scaffold.

In general, the putative binding modes of the 1*S*,5*R* series, where the tertiary nitrogen remains H-bonded to D83 in TMH3, force the C9-chain to point in a direction with close packing of side chains and limited access to water (Fig. S1†). By contrast, in the 1*R*,5*S* series, the chain points in a direction that is less constrained sterically and more hydrated (Fig. S1†) to make multiple, potentially favorable interactions with the receptor, either directly or through water bridges (as in **23**).[20] These differences in the solvation environment of the chain may have consequences in the binding affinities since electrostatic/H-bonding interactions can be compensated differently by the desolvation penalty, especially if the chain contains a polar substituent (*e.g.*, **14** and **15**). At the same time, hydrophobic groups in the chains of the 1*R*,5*S* series yield unstable structures due to the limited availability of nonpolar residues. This is the case of the enantiomer of **12**, which failed to stabilize in any of the simulations, frequently losing the H-bonding interaction with TMH3 and finding alternate modes of binding. One exception is **14b**; due to the chain length, it bends and interacts with TMH3, targeting the helix in regions also targeted by **12** and **15a** (Fig. S1†), hence its biased effect. In particular, the ester oxygens of **14b** are stabilized by direct H-bonds with Q60 (a residue found to be critical in imparting stereospecificity of **23**), whereas C76, V79, I80 and the nonpolar moiety of D83 stabilizes the chain through hydrophobic interactions (Fig. S1†). These observations are consistent with the fact that, although the 1*S*,5*R* series of compounds were generally more potent than their 1*R*,5*S* analogs, there were compounds in both series that did not recruit β-arrestin.

Conclusions

We formerly noted that H-bonding interactions provided by the C9*S*–OH of the phenylmorphan strongly influenced the interaction with MOR.[18,24] While we initially thought that the extreme G-protein bias for **13** and **15** could be due to such H-bonding interactions, a very similar bias profile for the C9-propyl-substituted **12** suggests this may not be the case. Interestingly, while the methyl ester **14a** has a relatively small bias factor reflecting its ability to recruit β-arrestin, its enantiomer **14b** shows a complete lack of β-arrestin recruitment. Although the 1*S*,5*R* series of compounds were generally more potent than their 1*R*,5*S* analogs, there were compounds in both series that did not recruit β-arrestin. Also, the stereochemistry at the C9 position was noted to be an important factor affecting the interaction of the 5-phenylmorphans with the MOR, and that was clearly indicated by an C9*S*-epimer **22** that was far less potent as a MOR agonist than its C9*R*-epimer **14a**.

In this series of 3-carbon chain analogs at C9, we have identified three compounds, all in the 1*S*,5*R*,9*R* series, that will be of interest for further study *in vivo*. These were **12** (3-((1*S*,5*R*,9*R*)-2-phenethyl-9-propyl-2-azabicyclo[3.3.1]nonan-5-

yl)phenol), **13** (3-((1*S*,5*R*,9*R*)-9-((*E*)-3-hydroxyprop-1-en-1-yl)-2-phenethyl-2-azabicyclo[3.3.1]nonan-5-yl)phenol), and **15a** (3-((1*S*,5*R*,9*R*)-9-(3-hydroxypropyl)-2-phenethyl-2-azabicyclo[3.3.1]-nonan-5-yl)phenol), which were found to be *ca.* 5, 3, and 4-fold more potent than morphine *in vitro*, respectively, have no detectable activity at KOR, and weak activity at DOR. Compounds **12**, **13**, and **15a** failed to recruit β-arrestin in two different assays for β-arrestin recruitment. Additionally, **12**, **13**, and **15a** display selectivity for the MOR, which would mitigate potential side effects that may be elicited by activating the other opioid receptors. Molecular dynamic simulations show that more direct engagement of TMH3 is essential to impart biased activity; the strong non-polar interactions between this helix and the 3-carbon spacer at C9 likely confers the extreme G-protein bias to **12** and **15a**.

Author contributions

The manuscript was written with contributions from all the authors, and all authors have given approval of the final version of the manuscript.

Abbreviations

EC	Extracellular
IC	Intracellular
ICL	Intracellular loop
ECL	Extracellular loop
TMH	Transmembrane helix
MOR	μ-Opioid receptor
cAMP	Cyclic adenosine monophosphate
DAMGO	[D-Ala2, *N*-Me-Phe4, Gly5-ol]-enkephalin
PDB	Protein Data Base

Conflicts of interest

The authors declare no competing financial interest. ESG, EB, FL, AEJ, and KCR are inventors on a patent assigned to NIH covering biased potent opioid-like agonists.

Acknowledgements

The work of ESG, EB, FL, AS, AEJ, and KCR was supported by the NIH Intramural Research Program (IRP) of the National Institute on Drug Abuse and the National Institute of Alcohol Abuse and Alcoholism. The work of SK, RC, and TEP was supported by DA018151 (to TEP) and GM008545 (to RC). The work of Y-SL and SAH was supported by the NIH IRP through the CIT and utilized the high-performance computer capabilities of the Biowulf HPC cluster at the NIH. The X-ray crystallographic work was supported by NIDA through an Interagency Agreement #Y1-DA1101 with the Naval Research Laboratory (NRL). NIH, DHHS. We thank Dr. John Lloyd (Mass Spectrometry Facility, NIDDK) for the mass spectral data.

References

1 Z. Rankovic, T. F. Brust and L. M. Bohn, *Bioorg. Med. Chem. Lett.*, 2016, **26**, 241–250.
2 K. M. Raehal, C. L. Schmid, C. E. Groer and L. M. Bohn, *Pharmacol. Rev.*, 2011, **63**, 1001–1019.
3 L. M. Bohn, R. J. Lefkowitz, R. R. Gainetdinov, K. Peppel, M. G. Caron and F.-T. Lin, *Science*, 1999, **286**, 2495–2498.
4 L. M. Bohn, R. R. Gainetdinov, F. T. Lin, R. J. Lefkowitz and M. G. Caron, *Nature*, 2000, **408**, 720–723.
5 S. M. DeWire, D. S. Yamashita, D. H. Rominger, G. Liu, C. L. Cowan, T. M. Graczyk, X.-T. Chen, P. M. Pitis, D. Gotchev, C. Yuan, M. Koblish, M. W. Lark and J. D. Violin, *J. Pharmacol. Exp. Ther.*, 2013, **344**, 708–717.
6 A. A. Altarifi, B. David, K. H. Muchhala, B. E. Blough, H. Akbarali and S. S. Negus, *J. Psychopharmacol.*, 2017, **31**, 730–739.
7 E. L. May and A. E. Jacobson, *Drug Alcohol Depend.*, 1989, **23**, 183–218.
8 L. S. Harris and E. L. May, *Drug Alcohol Depend.*, 1985, **14**, 227–232.
9 S. Engineer and S. Jennett, *Br. J. Anaesth.*, 1972, **44**, 795–802.
10 A. Dahan, A. Yassen, R. Romberg, E. Sarton, L. Teppema, E. Olofsen and M. Danhof, *Br. J. Anaesth.*, 2006, **96**, 627–632.
11 A. Manglik, H. Lin, D. K. Aryal, J. D. McCorvy, D. Dengler, G. Corder, A. Levit, R. C. Kling, V. Bernat, H. Hübner, X.-P. Huang, M. F. Sassano, P. M. Giguère, S. Löber, D. Da, G. Scherrer, B. K. Kobilka, P. Gmeiner, B. L. Roth and B. K. Shoichet, *Nature*, 2016, **537**, 185–190.
12 C. L. Schmid, N. M. Kennedy, N. C. Ross, K. M. Lovell, Z. Yue, J. Morgenweck, M. D. Cameron, T. D. Bannister and L. M. Bohn, *Cell*, 2017, **171**, 1165–1175.
13 X.-T. Chen, P. Pitis, G. Liu, C. Yuan, D. Gotchev, C. L. Cowan, D. H. Rominger, M. Koblish, S. M. DeWire, A. L. Crombie, J. D. Violin and D. S. Yamashita, *J. Med. Chem.*, 2013, **56**, 8019–8031.
14 A. Kliewer, A. Gillis, R. Hill, F. Schmidel, C. Bailey, E. Kelly, G. Henderson, M. J. Christie and S. Schulz, *Br. J. Pharmacol.*, 2020, **177**, 2923–2931.
15 A. Kliewer, F. Schmiedel, S. Sianati, A. Bailey, J. T. Bateman, E. S. Levitt, J. T. Williams, M. J. Christie and S. Schulz, *Nat. Commun.*, 2019, **10**, 367.
16 K. C. Rice, A. E. Jacobson, F. Li, E. Gutman and E. W. Bow, *U.S. Pat.* WO2019182950, 2019.
17 E. L. May and J. G. Murphy, *J. Org. Chem.*, 1955, **20**, 1197–1201.
18 A. C. Hiebel, Y. S. Lee, E. J. Bilsky, D. Giuvelis, J. R. Deschamps, D. A. Parrish, M. D. Aceto, E. L. May, E. M. Harris, A. Coop, C. M. Dersch, J. S. Partilla, R. B. Rothman, A. E. Jacobson and K. C. Rice, *J. Med. Chem.*, 2007, **50**, 3765–3776.
19 J. T. M. Linders, J. L. Flippen-Anderson, C. F. George and K. C. Rice, *Tetrahedron Lett.*, 1999, **40**, 3905–3908.
20 P. M. Truong, S. A. Hassan, Y.-S. Lee, T. A. Kopajtic, J. L. Katz, A. M. Chadderdon, J. R. Traynor, J. R. Deschamps, A. E. Jacobson and K. C. Rice, *Bioorg. Med. Chem.*, 2017, **25**, 2406–2422.

21 R. S. Crowley, A. P. Riley, A. M. Sherwood, C. E. Groer, N. Shivaperumal, M. Biscaia, K. Paton, S. Schneider, D. Provasi, B. M. Kivell, M. Filizola and T. E. Prisinzano, *J. Med. Chem.*, 2016, **59**, 11027.

22 F. J. Ehlert, M. T. Griffin, G. W. Sawyer and R. Bailon, *J. Pharmacol. Exp. Ther.*, 1999, **289**, 981–992.

23 D. Winpenny, M. Clark and D. Cawkill, *Br. J. Pharmacol.*, 2016, **173**, 1393–1403.

24 M. R. Iyer, Y. S. Lee, J. R. Deschamps, C. M. Dersch, R. B. Rothman, A. E. Jacobson and K. C. Rice, *Eur. J. Med. Chem.*, 2012, **50**, 44–54.

25 ThermoFisher Scientific, *Tango GPCR Assay System*, https://www.thermofisher.com/us/en/home/industrial/pharma-biopharma/drug-discovery-development/target-and-lead-identification-and-validation/g-protein-coupled/gpcr-cell-based-assays/tango.html.

26 G. Laroche and P. M. Giguere, in *G Protein-Coupled Receptor Signaling: Methods and Protocols*, ed. M. Tiberi, Springer Science+Business Media, LLC, Springer Nature, 2019, vol. 1947, pp. 257–267.

27 K. J. Sutcliffe, G. Henderson, E. Kelly and R. B. Sessions, *J. Mol. Biol.*, 2017, **429**, 1840–1851.